

FAULT DETECTION USING THE ZERO CROSSING RATE

By

C. C. Osuagwu
Department of Electronic Engineering,
University of Nigeria, Nsukka.

ABSTRACT

A method of fault detection based on the zero crossing rate of the signal, Z_1 , and the zero crossing rate of the first order difference signal, Z_2 , is presented. It is shown that the parameter pair (Z_1, Z_2) possesses adequate discriminating potential to classify a signature as good or defective. The parameter pair also carries considerable information about the underlying system structure and it is shown that the different clusters for the good and defective signatures in the (Z_1, Z_2) space are related to the excited system poles. The sensitivity of the (Z_1, Z_2) parameter pair to the dominant system poles makes the technique very effective in cases where the excited system resonances in the good and defective signatures are different.

1. INTRODUCTION

The fault detection problem is easy to state: Given a time series derived from a mechanism classify its state in the good/defective binary space. The key to fault detection is the extraction of a minimum feature set sufficiently sensitive to discriminate between the good and defective states under all operating conditions. The need for feature extraction arises because the input signal (the pattern in the pattern space) has large data and low information. The feature extractor is simply a mapping of the input signal from the pattern space into the low data, high information feature space. Feature extraction results, therefore, in drastic data compression [1].

Feature extraction can be carried out in the time, frequency or statistical domains. Compared to feature extraction in the frequency domain, time domain feature extraction is computationally simple [2]. The zero crossing rate of a finite time series (signature) is a time domain feature which gives an indication of the frequency concentration of energy in the signal power spectrum. This technique has been used in a variety of fields from speech processing to biomedical engineering [3]. Its use in discriminating between a good and defective signature is the objective of this paper.

1.1 THE THRESHOLD TEST AND DEFECT DETECTION

Given the zero crossing rate of a signal, can we classify that signal as coming from a good or defective mechanism? This is the question we wish to answer. A basic idea in all defect detection based on feature measurement is the threshold test illustrated in figure 1.

Three steps are involved in this test:
(i) a stored feature bound T defining the limits of

acceptable values for the mechanism in the good condition .

- (ii) the present feature value F extracted from the waveform under test.
- (iii) the actual decision step: if $F > T$, decide that the mechanism is defective, otherwise decide that it is good.

This three-step procedure was used in the work reported here. The input sequence of figure 1 is obtained from a Seta mechanism [4]. A description of the Seta mechanism is also given in the appendix. The features extracted are the zero crossing rate of the signal Z_1 and the zero crossing rate of the first differenced signal Z_2 . The thresholds are established by experimentation as shown in section 4.

2. BASIS FOR USING THE ZERO CROSSING RATE

The presence of high amplitude, short duration, quasi-periodic impacts in the Seta defect waveforms constitute time events whose basic relationship is determined by the impact repetition rate. The absence of these events in the good Seta waveform provides a sound basis for discrimination between a good and defective Seta mechanism. The amplitude structure of the Seta defect waveform (see figure 2a) can be decomposed into its constituent parts as shown in figure 2(b) and figure 2(c). The Seta diagnostic signal of figure 2 (a) can be viewed as the result of an amplitude modulation in which a Seta natural frequency of figure 2(b) act as the carrier and the periodic time varying amplitude of the diagnostic signal of figure 2(c) acts as the modulating signal. Therefore, it can be seen from figure 2(a) that the zero crossing rate of the diagnostic signal gives a measure of the domain system resonance excited by the period sequence

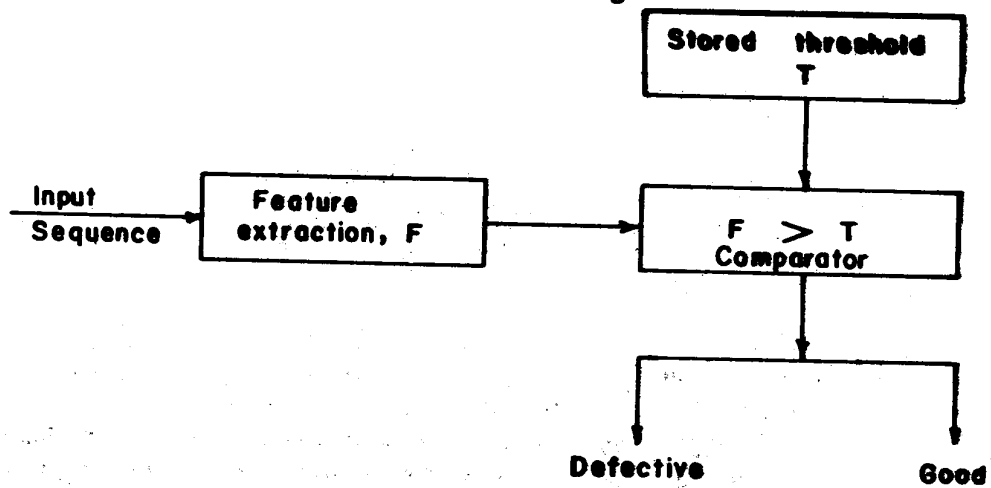
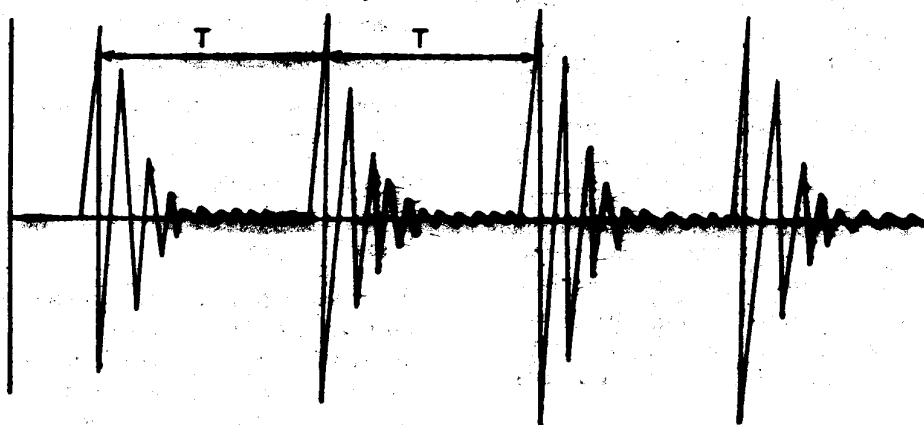
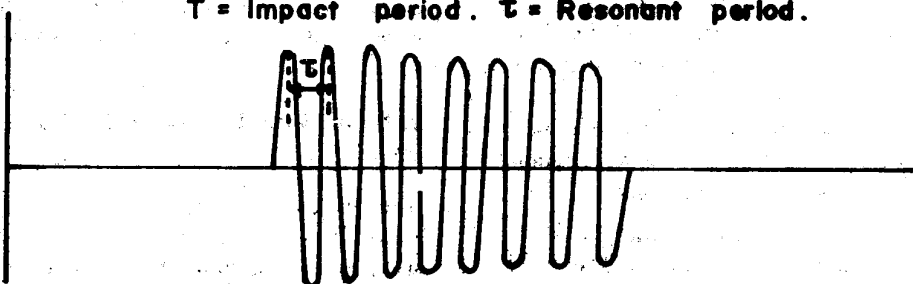


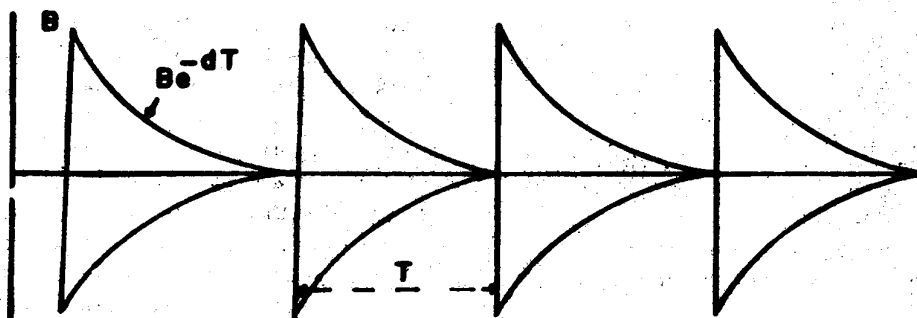
Fig. 1: Threshold test – basis for defect detection.



(a) Seta defect waveform.
 T = Impact period. τ = Resonant period.



(b) Excited seta resonant frequency.



(c) Seta amplitude profile.

Fig. 2: Decomposition of a seta defect waveform into its constituent parts.

of impact in the defective case. Since the impact information carried in the envelope structure of the Seta waveform as shown in figure 2(c), the zero crossing rate contain no direct information about the impact frequencies due to defect. In the good case, the zero crossing rate of the diagnostic signal gives a measure of the dominant system resonance excited by the random input excitation. The basis of the technique, therefore, is that if the excited resonances in the good and defective states, are sufficiently different, the zero crossing rates in the two cases will differ markedly.

2.1 DEFINITION OF ZERO CROSSING RATES

The zero crossing rate (ZCR) is obtained by infinitely clipping the waveform using the Sgn operator and the following relations:

$$z_1 = \sum_{i=1}^N [1 - \text{Sgn}(X_{i+1}) \text{Sgn}(X_i)]/2$$

$$z_2 = \sum_{i=1}^N [1 - \text{Sgn}(\psi_{i+1}) \text{Sgn}(Y_i)]/2$$

$$Y_i = X_{i+1} - X_i$$

Where $\text{Sgn}(X_i) \begin{cases} 1, X_i > 0 \\ -1, X_i < 0 \end{cases}$ (1)

A simple example can be used to illustrate the application of the zero crossing rate. Consider the values obtained by sampling the waveform of figure 3 at uniform intervals

as shown by the dotted points. The sequence x_i obtained from the sampled values by the application of the Sgn operator:

$$\text{Sgn}(X_i) \begin{cases} 1, X_i > 0 \\ -1, X_i < 0 \end{cases} \quad (2)$$

is

$$X_i \quad [1, -1, 1, -1, 1, -1, 1, -1, -1, -1, 1, 1, 1, 1, 1, 1, 1, -1, 1, -1, 1, -1, 1, -1, 1]$$

Applying equation 1 to the sequence x_i we obtain

$$z_1 = \sum_{i=1}^{25} [1 - \text{Sgn}(X_{i+1}) \text{Sgn}(X_i)]/2 \quad (3)$$

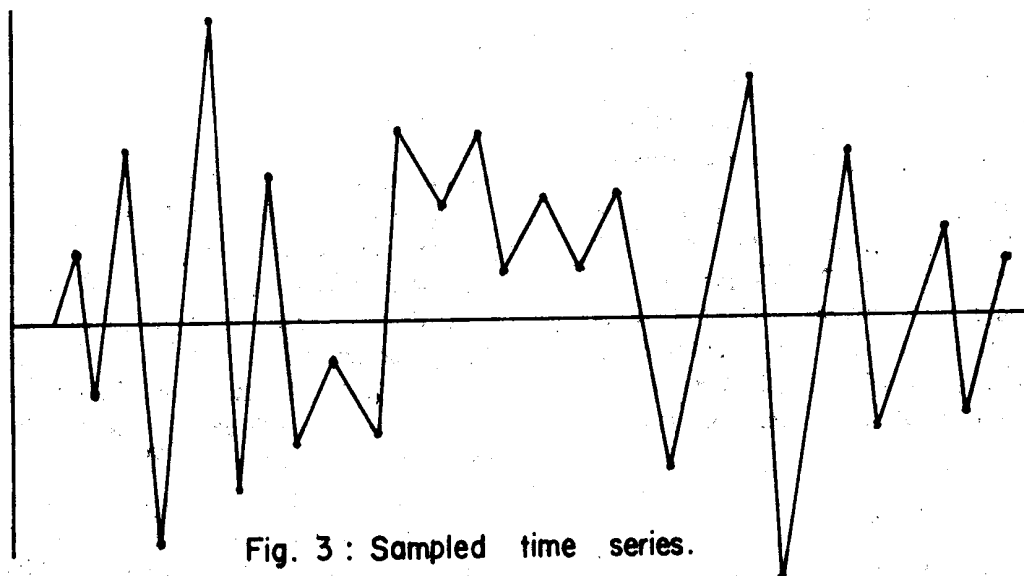
$$z_1 = \frac{32}{2} = 16$$

Hence the waveform of figure 3 has a zero crossing count of 16. If the waveform length is 4 milliseconds, then the zero crossing rate Z_1 becomes

$$z_1 = \frac{16}{4} = 4 \text{ Zero crossings/millisecond.}$$

2.2 ZERO CROSSING RATE OF THE DIFFERENCE SIGNAL

Obtaining the zero crossing rate of the difference signal is equivalent to passing the signal through 2 linear high pass filter and then calculating the zero crossing rate of the filtered signal. In this paper



only the first order difference Signal is used; higher order difference signals were not considered.

Consider the difference signal

$$Y_i = X_{i+1} - X_i \quad (4)$$

Taking the Z transform of eqn (4) we obtain

$$Y(Z) = ZX(Z) - X(Z)$$

$$\frac{Y(Z)}{X(Z)} = H(Z) = Z - 1 \quad (5)$$

Now the frequency response of this filter is

$$H(e^{j\omega T} - 1) \quad (6)$$

$$= \exp\left(\frac{j\omega T}{2}\right) \left[\exp\left(\frac{j\omega T}{2}\right) - \exp\left(-\frac{j\omega T}{2}\right) \right]$$

$$|H(j\omega)| = 2 \sin \frac{\omega T}{2} \quad (7)$$

$$\therefore |Y(j\omega)| = 2 \sin \frac{\omega T}{2} |X(j\omega)| \quad (8)$$

Equation 8 shows that the differencing operation results in emphasizing the high frequency content of the signal since $Y(j\omega) = 0$ at $\omega = 0$ and attains a maximum at $\omega = \pi/T$. The Seta/signal in the good state is random and therefore can be characterized as a wide-band signal. With the onset of defect, the Waveform changes from being random to being impact dependent. Since these impacts are low frequency events, the defective. Waveform can be characterized as narrow band. Hence as the Seta waveform changes from good to defective, its frequency characteristics changes from wide-band (relatively high frequency) to narrow band (relatively low frequency). Thus the underlying system structure is expected to exhibit low frequency resonances due to the onset of defect.

The zero-crossing rate of the difference signal will tend to emphasize the high frequency poles of the Seta mechanism because of the high pass filtering operation and is therefore expected to result in higher ZCR value compared to the zero crossing rate of the signal which will emphasize the resonant frequencies excited by the low frequency impacts due to defect.

3. ANALYSIS METHOD

The Seta waveform, band pass filtered in the range 5Hz to 1 kHz and sampled at 3.2 kHz is divided into groups of fifty non-overlapping signatures where each signature has a 15mm duration. For each signature, the zero crossing rates of both the signal and the difference signal are computed. The mean values of these features are then used as the discriminating parameter, In order to obtain reliable results, it is essential to consider a large number of signatures. In the total number of signatures analysed varied between 450 and 550.

4. RESULTS

Figure 4 shows a typical plot of the average zero crossing rate of the difference signal against the average zero crossing rate of the signal. As can be seen from the plot, the ZCR values for the good seta, data tend to lie within a fairly tight cluster labelled A in the plot. Hence a Seta data with, (Z_1, Z_2) values above, the threshold value (19, 21) is definitely good in the defective case, the dispersion in the ZCR values is Wider as indicated by the cluster labelled C. Thus a Seta data with (Z_1, Z_2) values below the threshold value (17, 19) is definitely defective, ZCR values in the range $17 < Z_1 < 20$ and $19 < Z_2 < 21$ cannot be used to classify the Seta data as either good or defective. This range indicates a zone of overlap of values between the good and defective ZCR values and is labelled B in figure 4. It is interesting to note that it is only the Seta, 6 data whose ZCR values lie in this zone of overlap.

5. EXPLANATION OF RESULTS

It is necessary to explain:

- (i) why there is a wide dispersion in the (Z_1, Z_2) cluster for the defective case.
- (ii) why only the ZCR values of the Seta 6 data lie in the zone of overlap even though the speed of operation of the Seta 6 data (1920) rpm) is less than the speed of operation of the Seta 7 data (3000rpm).
- (iii) why the best separability in the (Z_1, Z_2) space is obtained for the Seta 13 data operated at the speed of 1000 rpm,

As was mentioned in section 1, the zero crossing rates give information about the underlying system structure (system resonances) of the mechanism under study. The dispersion in the (Z_1, Z_2) value in the defection case may be due to differences in the resonances excited. For example, the Seta 13 defective ZCR values show two tight cluster at low (Z_1, Z_2) rates and three fairly dispersed values. This will suggest the existence, in the underlying structure, of two low frequency resonances compared to the other excited rates. Similarly the region of overlap can be explained by assuming that the resonances excited by the Seta 6 data, is essentially the same in the good and defective states.

To find out the nature of the underlying system structure, it is necessary to separate by deconvolution the system impulse response, $h(t)$,

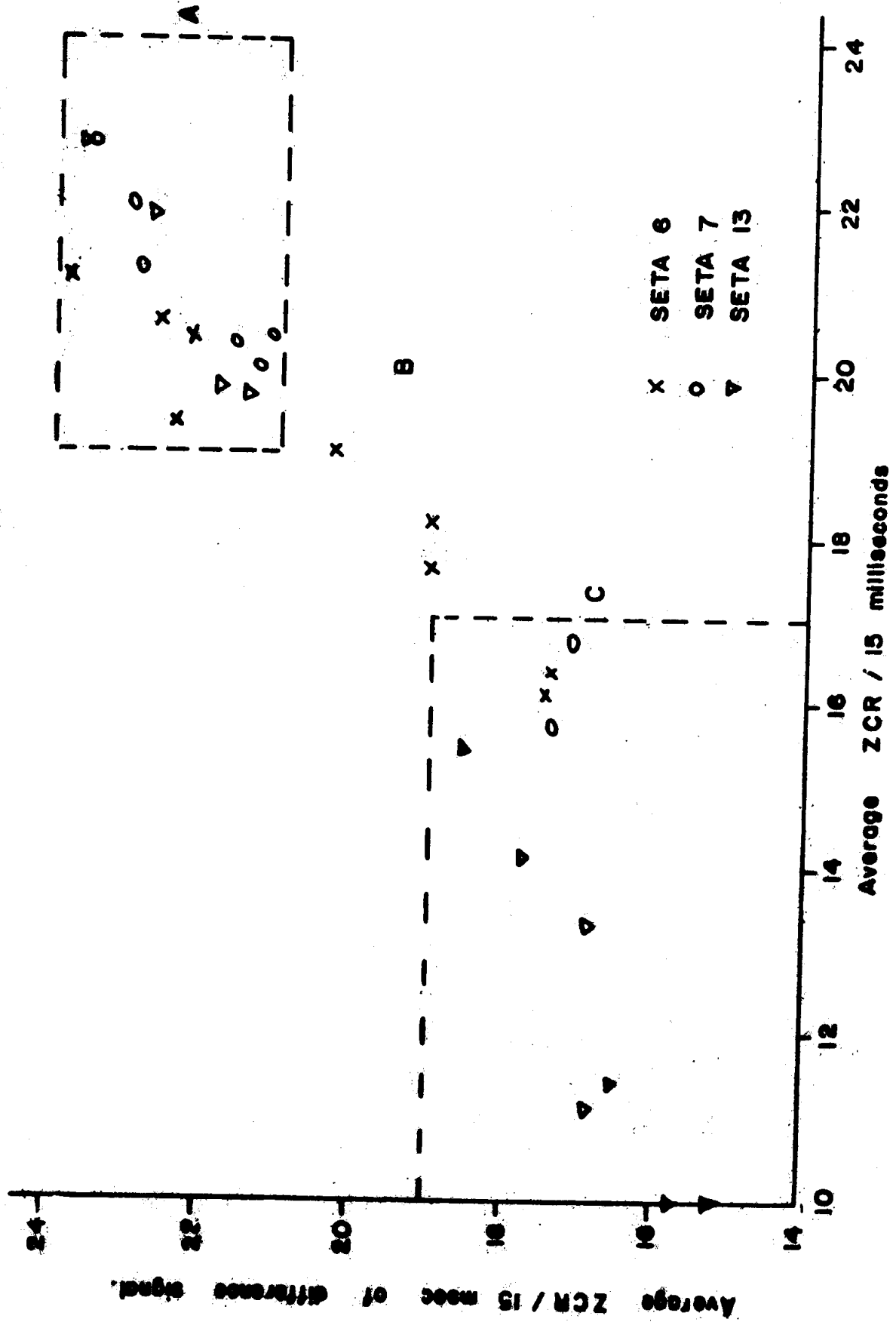


FIG. 4: Plot of Z2 against Z1

from the input excitation $x(t)$ since the acquired diagnostic signal yet is given by

$$y(t) = x(t) * h(t) \quad (9)$$

where $*$ denotes convolution,

Now, since convolution in the time domain is equivalent to multiplication in the frequency domain, the power spectrum of the signal is given by the relation

$$|Y(f)|^2 = |X(f)|^2 |H(f)|^2 \quad (10)$$

Taking the logarithm of both sides of equation 10 gives

$$\log|Y(f)|^2 = \log|X(f)|^2 + \log|H(f)|^2 \quad (11)$$

If the system transfer function $H(f)$ resides in a sufficiently different frequency band from the input excitation $X(f)$, we can use linear filtering to separate the additive components of equation 11. That is the basis of homomorphic deconvolution or homomorphic filtering [5]. Using homomorphic filtering, the system transfer function can be obtained in the good and defective conditions.

5.1. HOMOMORPHED LOG POWER SPECTRUM

Figure 5 shows the homomorphed log power spectrum of the good Seta waveform superimposed on that of the defective waveform. From figure 5(a), it can be seen that 'the same resonances are excited in the good and defect states and that the energies at the excited resonances are the same except at the system pole at 562.5 Hz where the energy in the defect spectra is higher than that for the good spectra. Hence the overlap noticed in the ZCR plot for the Seta 6 data is caused by the fact that the same system resonances are excited with the same energies in both the good and defect states.

From figure 5(b) it can be seen that the resonance peaks at 500 Hz and 825 Hz in the good Seta 7 data have been replaced by a dominant resonant frequency due to defect centred at 525 Hz in the defect data. The concentration of energy in this resonant frequency due to defect is higher than the energies in the resonant peaks at 500 Hz and 825 Hz in the good Seta data. Indeed over all the excited resonances, the energies in the defective power spectra are greater than that in the good spectra. For this condition, where the defect excites a new resonant frequency with a large energy concentration, good separability exists for the good and defect waveforms in the (Z_1, Z_2) space. The nearness of the new resonant frequency due to defect (525 Hz) to the resonant frequency at 500 Hz in the good case does not seem to matter.

From figure 5(c), it can be seen that two low frequency resonances are excited by defect in the Seta 13 data. These occur at 125 Hz and 475 Hz with large energy concentrations compared to the system poles at 250 Hz and 562.5 Hz in the good Seta 13 data. In this case, too, very good separability exists in the (Z_1, Z_2) space and hence accurate defect detection results.

5.2 DISCUSSION OF RESULTS

The results show that the key to separability of the good and defect waveforms into two distinct clusters in the (Z_1, Z_2) space is due to the following:

- (i) the excitation of new resonant frequencies due to defect,
- ii) the large concentration of energy in the defect induced resonances compared to the energy in the excited system poles in the good state.

It is because the Seta 6 data did not excite any new resonances and the concentration of energy in the system poles in the defective state was almost the same as in the good state, that misclassification of a Seta state in the (Z_1, Z_2) space resulted. This misclassification potential is shown in figure 4 by the region of overlap (B) between the good state cluster (A) and the defect state cluster (C).

The best separability between the good and defect Seta waveforms in the (Z_1, Z_2) space was obtained for the Seta 13 data. Here we find that the impacts due to defect excited the highest number of low frequency resonances; and that these new resonant frequencies are associated with high concentration of energies in the power spectrum. Clearly then, the zero crossing rates carry considerable information about the underlying system structure (poles of the system transfer function) and are very sensitive in detecting new resonant frequencies due to defect.

6. CONCLUSION

The zero crossing rates have been shown to be effective time domain discriminant features for detecting incipient defect in a Seta mechanism. This technique should prove very effective for detecting faults in any mechanism where the defect excites new high energy resonances compared to the resonances excited in the good state. The zero crossing rate is a very easy technique to use and in addition gives considerable information about the underlying system structure. The result also shows that the zero crossing rates should not be used as discriminating features for systems where the defect excites no new resonances in the mechanism.

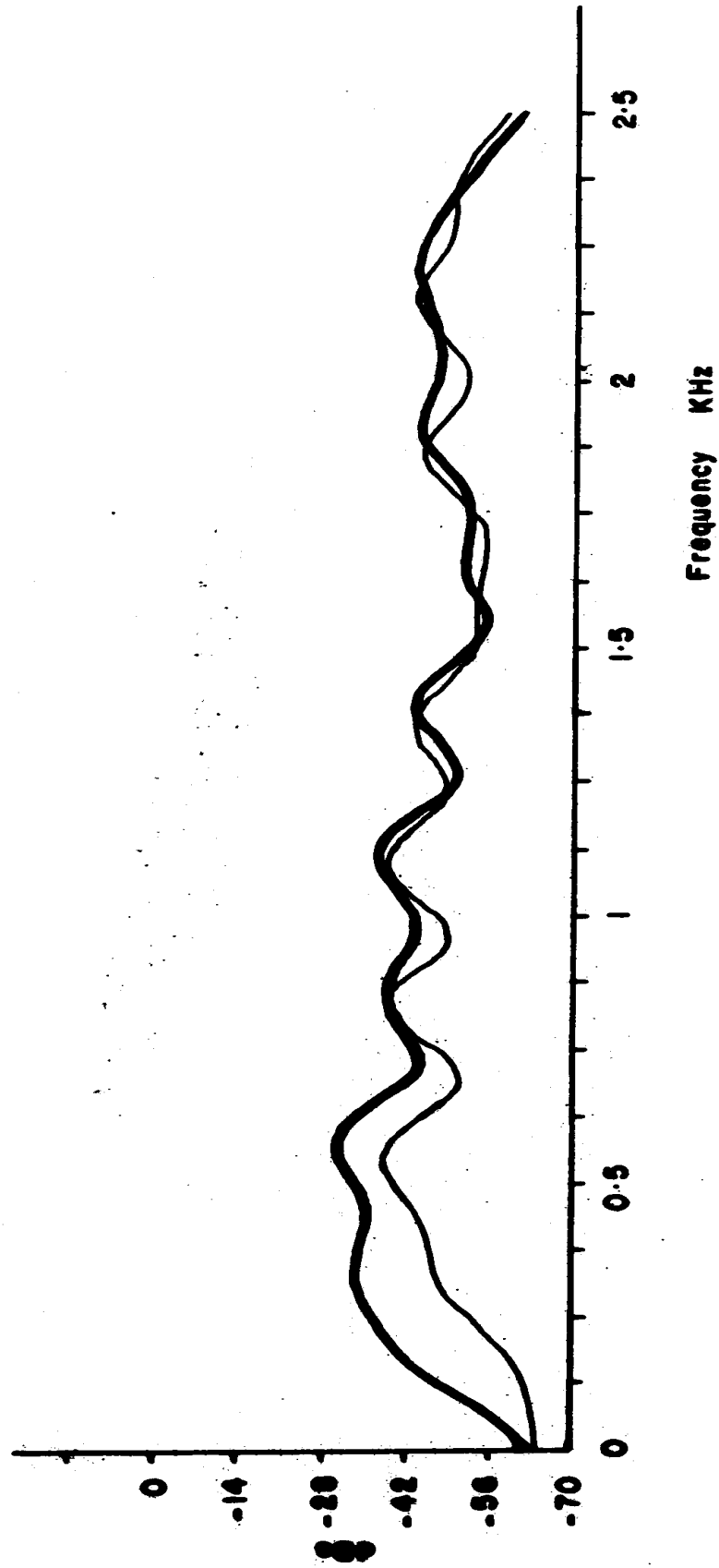


Fig. 5(a): Homomorphed log power spectrum for seta 6

— Defective spectrum, — Good spectrum.

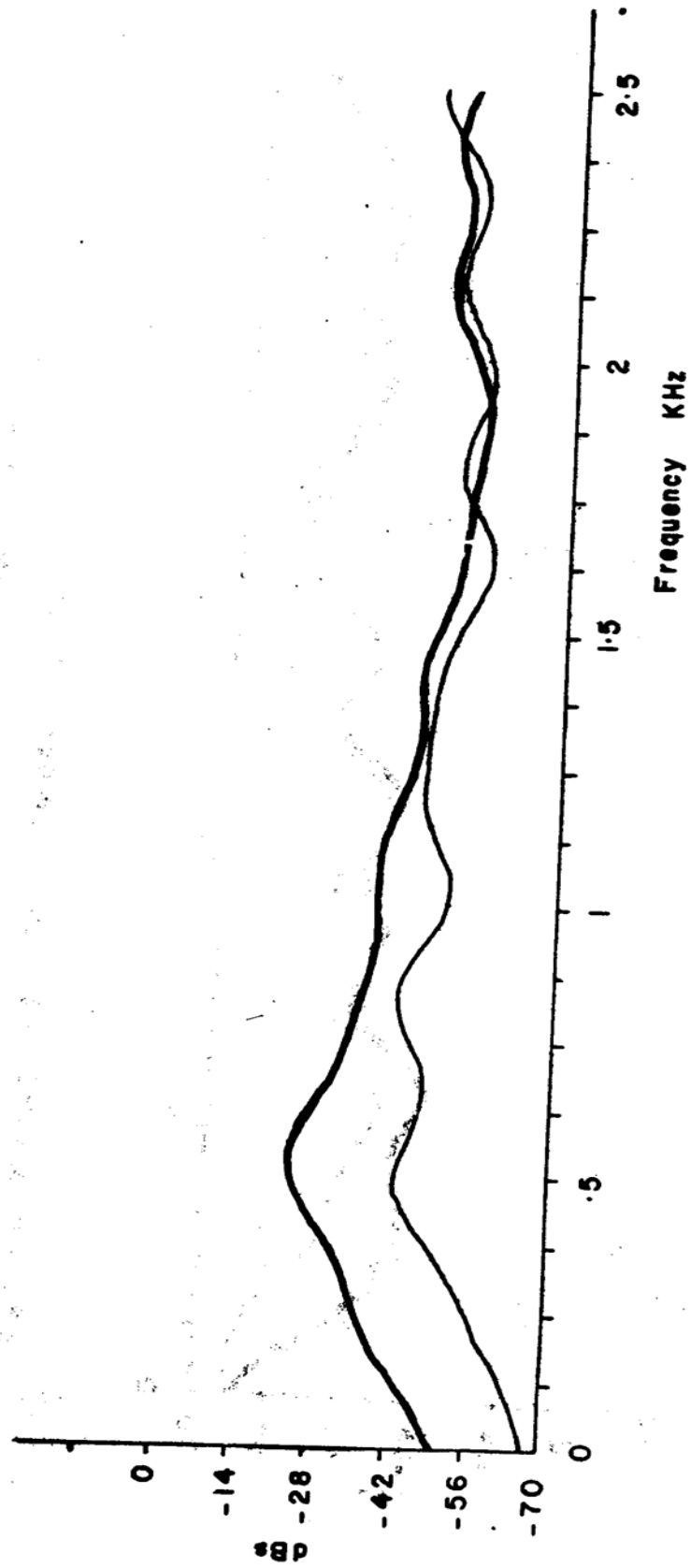


Fig.5 (b): Homomorphed log power spectrum for seta 7.
—— Defective spectrum, - - - Good spectrum.

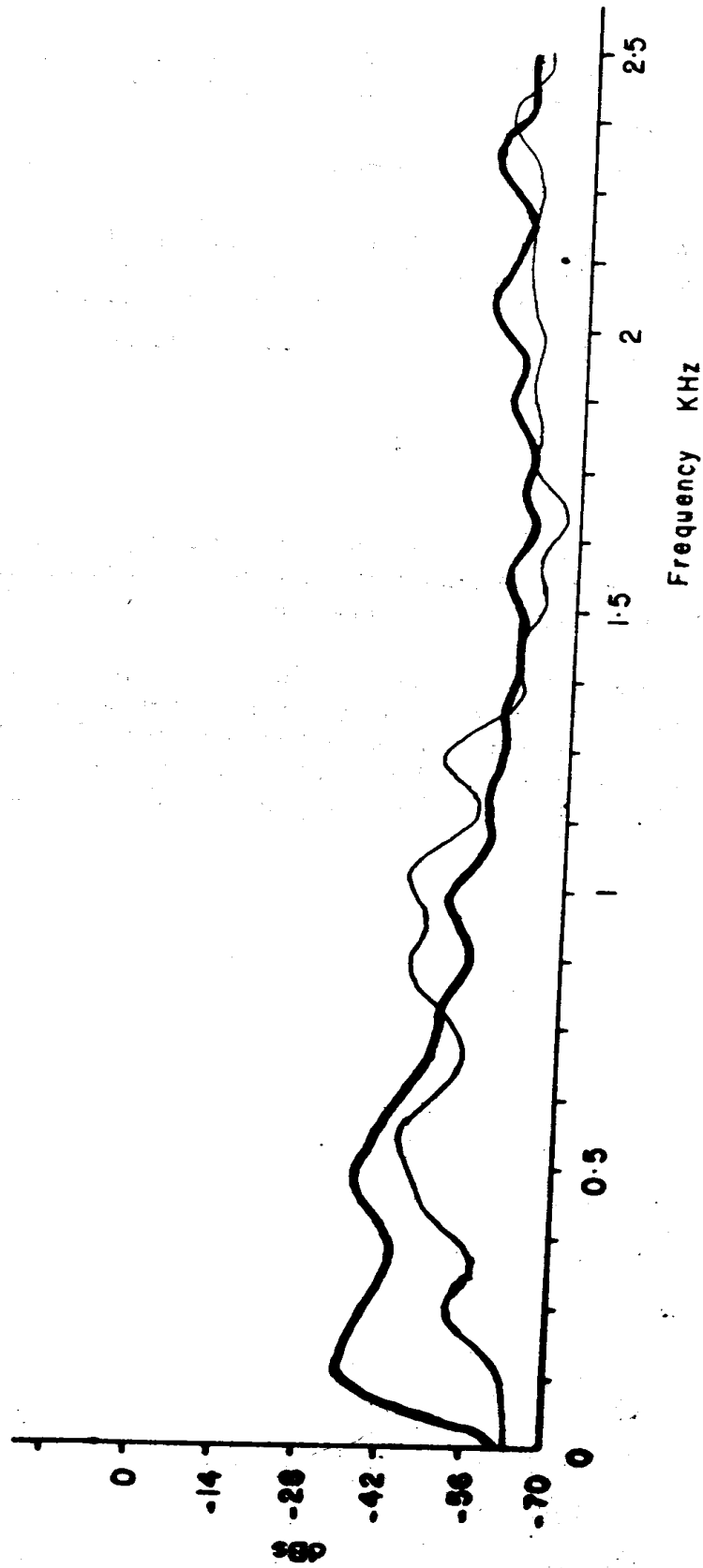


Fig. 9(a): Homomorphed log power spectrum for seta 13.
—— Defective spectrum, - - - Good spectrum.

REFERENCES

1. NAGY, G., "State of the Art in Pattern Recognition", *Proc. IEEE*, Vol. 56, 'No. 5 pp 836 - 862. May, 1968.
2. OSUAGWU, C. C., "Automatic Diagnosis of Rolling Element Incipient Defect Using the Average Magnitude Difference Function". *International Symposium on Electronic Devices Circuits and Systems*, Vol. 2, pp. 540 - 542, Dec. 1987.
3. KEDEM, B., "Spectral Analysis and Discrimination by Zero-Crossing" *Proc. IEEE*. Vol. 14, No. 11, pp1477 - 1493, Nov., 1986.
4. OSUAGWU, C. C., THOMAS, D. W., "Effect of Inter-Modulation and Quasi-Periodic Instability in the Diagnosis of Rolling Element Incipient Defect". *Journal of the ASME – Mechanical Design (Special Issue: Mechanical Signature Analysis)* Vol. 104, No.2.; pp 296 -301, April, 1982.
5. OPPENHEIM, A. V., SCHAFER. R. W., *Digital Signal Processing* Prentice – Hall Inc., New Jersey. 1975.

APPENDIX**SETA MECHANISM**

The Seta four ball life resting machine is generally used to study lubricant properties which may affect bearing life and to evaluate the life of rolling elements. In this study, its ability to produce the same type of failure as ball bearing quickly and relatively inexpensively is utilized to obtain data on fatigue failure under rolling contact condition

The Seta mechanism consists of four balls, a thin tufnol cage used to separate the three lower balls and a ball cup which holds the three lower balls. The shaft holding the upper ball is driven by an electric motor and tests can be conducted up to a speed of 3000 rpm. The rolling elements are loaded through thrust bearing by hanging static weights an appropriate distance from the fulcrum of a lever mechanism. A high loading of 600kg was used in the test in order to accelerate the time to produce the first fatigue spall.